AIP | Applied Physics Letters

Structural characterization of CdSe/ZnS quantum dots using medium energy ion scattering

M. A. Sortica, P. L. Grande, C. Radtke, L. G. Almeida, R. Debastiani et al.

Citation: Appl. Phys. Lett. **101**, 023110 (2012); doi: 10.1063/1.4734686
View online: http://dx.doi.org/10.1063/1.4734686
View Table of Contents: http://apl.aip.org/resource/1/APPLAB/v101/i2
Published by the American Institute of Physics.

Structural characterization of CdSe/ZnS quantum dots using medium energy ion scattering

M. A. Sortica,[1,a)] P. L. Grande,[1] C. Radtke,[2] L. G. Almeida,[1] R. Debastiani,[1] J. F. Dias,[1] and A. Hentz[1]
[1]*Instituto de Física, UFRGS, Av. Bento Gonçalves, 9500, 91501-970, Porto Alegre, Rio Grande do Sul, Brazil*
[2]*Instituto de Química UFRGS, Av. Bento Gonçalves, 9500, 91501-970, Porto Alegre, Rio Grande do Sul, Brazil*

(Received 31 May 2012; accepted 18 June 2012; published online 11 July 2012)

In the present work, we have analyzed CdSe/ZnS core-shell quantum dots by medium energy ion scattering (MEIS), which is a powerful technique to explore the synthesis, formation, stability, and elemental distribution of such core-shell structures, along with other auxiliary analytical techniques. By comparing different quantum-dot structural models spectra with the experimental MEIS data, we were able to obtain some sample structural information. We found that, despite the well known non stoichiometric Cd:Se ratio, the core is stoichiometric, and there is an excess of cadmium distributed in the shell. © *2012 American Institute of Physics*. [http://dx.doi.org/10.1063/1.4734686]

Compound quantum dots (QDs) are promising materials already present in many fields of modern technology. Moreover, their electrical, optical, and magnetical properties can be tuned by adjusting their size, composition, and stoichiometry. For that reason, techniques capable to perform elemental profiling and size evaluation, with resolution better than 1 nm, are extremely important. One of the most studied quantum dots is the CdSe nanocrystal, coated by a ZnS, ZnSe, or CdS thin shell.[1]

Medium energy ion scattering (MEIS) is an ion beam analysis technique, similar to Rutherford backscattering spectrometry (RBS)[2] but with a much higher energy resolution, capable to perform quantitative depth distribution with subnanometric resolution[3,4] even for light elements in graphene.[5] For that reason, MEIS has been recently used for nanostructures characterization, to determine size distribution of nanoparticles, geometric shapes, composition, stoichiometry and, its most promising application, elemental distribution inside the QDs, which is hardly achieved by any other analytical technique.[6–8]

In this work, we studied sizes and elemental distribution of CdSe/ZnS core-shell quantum dots,[9] using MEIS in connection with other characterization techniques. CdSe/ZnS QDs are very suitable for MEIS analysis, since all elements correspond to well separated peaks in the energy spectrum when a few hundred keV He ions are used. Auxiliary techniques are also used to validate and to reduce the uncertainties of the MEIS analysis. In this way, we use transmission electronic microscopy (TEM) to visualize the QDs crystalline structure and the corresponding size distribution. Through RBS and particle induced X-ray emission (PIXE), we determined and check the overall ratio among elemental concentrations in the sample. Finally, the full analysis of the MEIS spectra in different scattering angles using the simulation software PowerMeis (Ref. 6) allows the determination of Cd and Se distributions inside the QDs.

Commercial CdSe/ZnS QDs, stabilized by trioctylphosphine oxide (TOPO), the EviDots ED-C11-TOL-0620 Maple Red-Orange from Evident Technologies, were used in this work. These QDs came diluted in toluene at the concentration of 2.2 mg/mL. This product has the advantage of having a monodisperse size distribution. This solution presents absorption and emission peaks at 585 nm and 612 nm, respectively, which correspond to a CdSe nanocrystal with 5.16 nm in diameter.[10] The samples were prepared by further diluting the solution in toluene down to a concentration of 3.82 μg/mL. For MEIS and RBS experiments, a droplet of this solution was applied to the surface of a $\langle 100 \rangle$ silicon wafer, covering an area of 100 mm^2. Subsequently, the samples were mounted on a spinner for 5 min, to spread the particles over the surface during the solvent evaporation. For the TEM images and the PIXE experiments, different substrates were used. For the TEM images, the Si substrate was replaced by a copper-carbon grid specially designed for electronic microscopy purposes. In the case of PIXE, the solution was deposited over a carbon tape instead of silicon, in order to avoid the interference of the intense Si K_α peak with the much less intense P K_α peak from the TOPO buffer.

MEIS experiments were performed at the MEIS experimental set, connected to a 500 kV ion accelerator, at the Laboratory of Ion Implantation of IF-UFRGS, with a He^+ beam of 200 keV. Backscattered ions are analyzed by an electrostatic toroidal system mounted at 60° with respect to the incident beam direction. Subsequently, they reach a set of two microchannel plates where a cloud of secondary electrons is generated, accelerated, and then detected by a position-sensitive detector. In this way, the system provides a two-dimensional spectra relating the energy and scattering angle of the particles with the number of events. The overall energy resolution achieved in these experiments was 800 eV when a 200 keV He^+ ion beam was employed. The data analysis consists in converting the two-dimensional data into one-dimensional energy spectra by summing up a wide angular range. The one-dimensional energy spectra obtained

[a)]Electronic mail: mausortica@gmail.com.

are analyzed by the PowerMeis code.[6] Contrary to other codes,[11] PowerMeis simulates the energy spectra of the backscattered particles by taking into account the full structure of the QDs: shape, composition, size distribution, and areal density. The QD structure is designed and stored in a 3D matrix, which is used as input to perform the full 3D Monte-Carlo integration. Further details can be found in the PowerMeis user's manual.[12]

RBS experiments were carried out with 2 MeV He^{2+} ions and typical currents of 15 nA at the target. Backscattered particles were detected by two surface barrier detectors placed at $+10°$ and $-10°$ with respect to the beam incident direction. Since Cd, Se, and Zn are clearly resolved in the RBS spectrum, the ratio between the concentrations of these elements can be obtained straightforwardly.[2] Since neither RBS nor MEIS can resolve the signals from sulfur (QDs) and phosphorus (TOPO buffer), PIXE experiments were carried out in order to find the ratio between P and S. A 2 MeV proton beam with currents of about 2 nA was employed in the experiments. Characteristic X-rays were detected by a Si(Li) detector placed at 45° with respect to the incident beam direction. The spectra were analyzed with the GUPIX software package.[13] Finally, TEM images were obtained with a JEM 2010 microscope (JEOL) from the Electronic Microscopy Center at UFRGS (CME - UFRGS).

For MEIS simulations, we used an atomic density of 3.66×10^{22} atoms/cm^3 and of 5.05×10^{22} atoms/cm^3 for CdSe core and ZnS shell, respectively. The compounds are configured in order to keep the global stoichiometry of the sample (Table I), and to take into account all the isotopes of cadmium, zinc, and selenium. The energy-loss factors were obtained from the Ziegler's Stopping and Range of Ions in Matter tables (SRIM 2011)[14] and the straggling values were calculated from Yang-O'Connor's correction of Chu's formula.[15] In addition, we used the exponentially modified gaussian (EMG) model for the energy loss distribution.[16] The single collision parameter for the EMG function was obtained from CasP.[16,17]

In Figure 1(a), we show one of the TEM images used to measure the QDs diameter distribution along with a higher resolution image, where the crystalline structure of the CdSe nucleus can be seen.

The core-shell structure of the QDs cannot be observed in all images due to the low contrast with the carbon background. The mean diameter evaluated from TEM images is 5.3 ± 0.5 nm. Despite the fact that the contours of the particles are not well defined in these images, the TEM results agree well with the mean nucleus diameter of about 5.16 nm, calculated from its emission peak from the fluorescence spectrum. We can also observe the nuclei are practically

TABLE I. Elemental fractions determined by RBS and PIXE.

Element	Fraction
Cd	0.19
Se	0.08
Zn	0.31
S	0.38
P	0.04

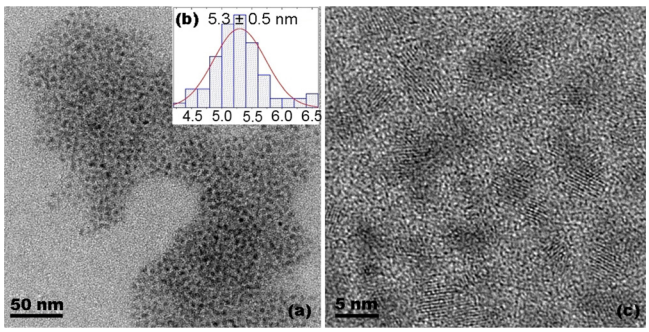

FIG. 1. Transmission microscopy image of the CdSe/ZnS QDs. (a) Large area to determine the size distribution of QDs (b) Histogram of QDs diameters. (c) Larger magnification to show the nanocrystals.

spherical and their diameters appear to be fairly uniform along the sample.

The overall stoichiometry of the sample was cross-checked by RBS, with the S:P ratio analyzed by PIXE. The results are summarized in Table I, resulting in a overall ratio of Cd:Se = 0.69:0.31 and Zn:S = 0.45:0.55. In fact the non-stoichiometry of CdSe was previously reported and depends on the preparation method and reaction time.[9]

We investigated the QDs internal structure by fitting the MEIS energy spectra at different scattering angles with results from the PowerMeis software. In Figure 2, we show the experimental and simulated 2D map of ion scattering intensities as a function of the scattering angle and energy.

As can be observed from this figure, except for the case of S and P, the scattering intensities are well separated, corresponding to bands indicated by each chemical element. The scattering angle dependence of each band depends mostly on the kinematical factor between the projectile and the target atom (the heavier the element, the weaker the angular dependence) but also on the spatial distribution of each element. From the full 2D spectrum, we select a small angular region (of about 2.5°) where the scattering angles are summed to generate a 1D energy spectrum. We have taken two energy spectra centered at 120° and 128° of scattering angle. We have avoided the use of smaller scattering angles,

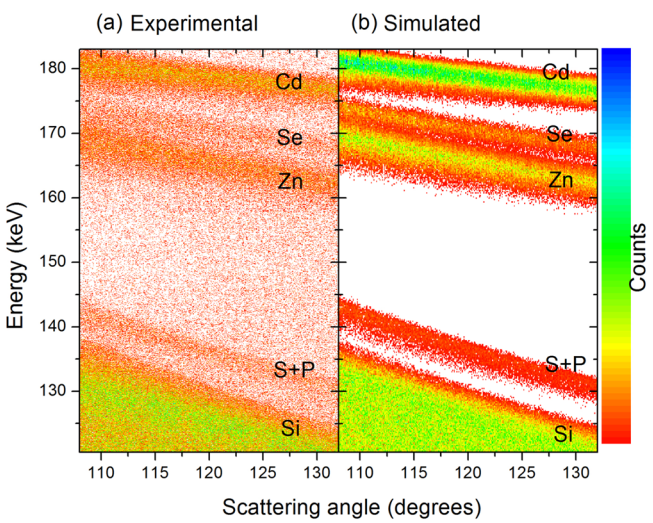

FIG. 2. Two dimensional map of the He^+ scattering intensities as a function of the scattering angle and energy. (a) Experimental and (b) simulated MEIS spectra of CdSe/ZnS QDs on a silicon surface.

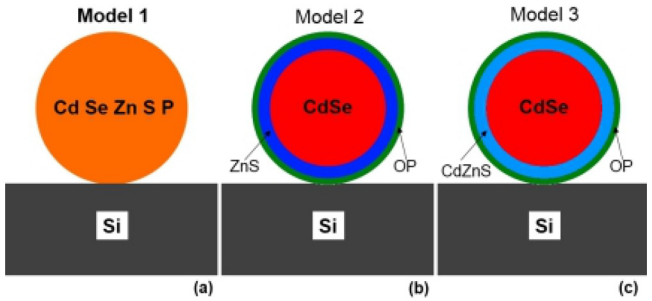

FIG. 3. Models of QDs used for MEIS spectra analysis with the software PowerMeis. (a) Homogeneous quantum dot representation, (b) core-shell CdSe/ZnS model, covered by a OP layer (that represents TOPO), and (c) core-shell CdSe/CdZnS model.

corresponding to grazing outgoing directions, since they give less information on the core-shell analysis and depend strongly on QDs neighborhood. By using the TEM, RBS, and PIXE data together, we built different structural models of spherical QD's on silicon surface, by fixing the total amount of elements according to Table I. Three models are discussed in this work, as shown in Figure 3.

The first model is a homogeneous sphere, composed by Cd, Se, Zn, S, and P (Figure 3(a)). The second one is a spherical core of CdSe with a shell of ZnS covered by a thin layer of OP, representing the TOPO stabilizer (Figure 3(b)). Figure 4 shows the comparison between the simulated (models 1 and 2) and experimental energy spectra.

An inspection of this figure shows a noticeable difference between these models, mainly regarding the shapes of Cd and Zn peaks. This confirms the capability of the present MEIS technique to identify different core-shell structures with the present energy resolution. Moreover, since no model seems to fully agree with the experimental data, there is room to optimize the core-shell parameters. Looking at the simulated spectrum of the core-shell model, we can observe that while the position of the Se peak agrees with the experiment, the leading edge of Cd peak is shifted towards lower energies and the whole peak is narrower, indicating the Cd is

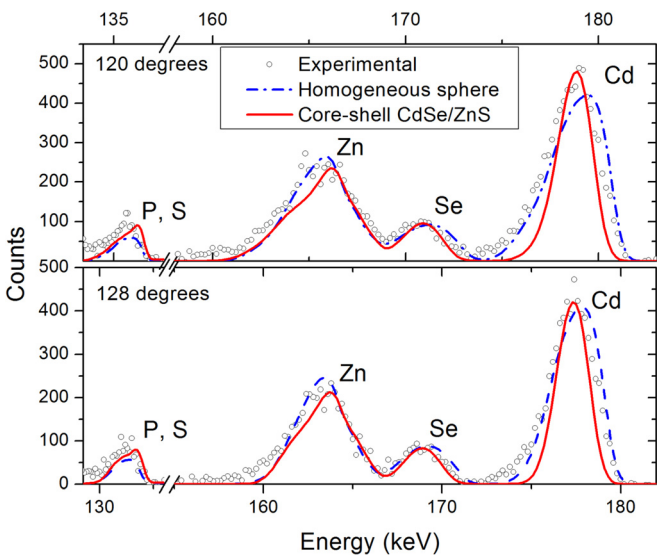

FIG. 4. Simulated MEIS energy spectra for a homogeneous CdSeZnS QD (dashed-line) and a core-shell CdSe/ZnS QD (solid-line) in comparison with present experimental data at two different scattering angles.

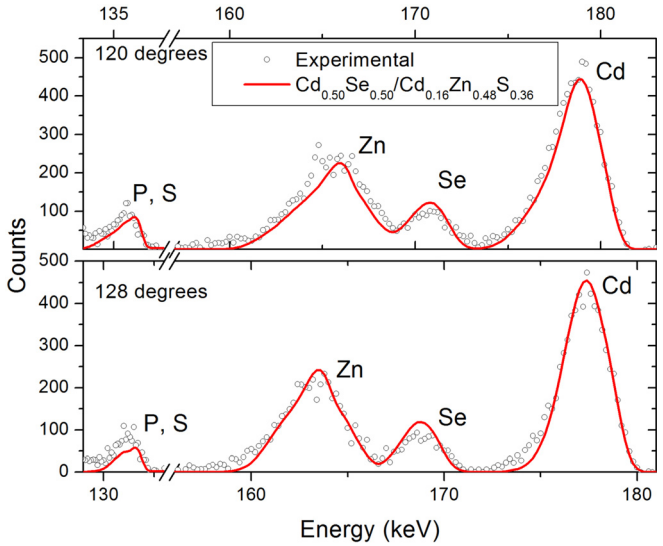

FIG. 5. Simulated MEIS energy spectra for stoichiometric CdSe core and Cd enriched ZnS shell (solid-line) in comparison with present experimental data at two different scattering angles.

also present in the shell. Since our sample has a CdSe overall concentration of about 69% of Cd and 31% of Se, we built a QD model with a stoichiometric CdSe nucleus and a Cd enriched shell of ZnS (CdZnS) (Figure 3(c)). The cadmium distribution outside of the nucleus was recently observed through extended X-ray adsorption fine structure (EXAFS) combined with diffraction anomalous fine structure (DAFS).[18] For this model, a new fitting of the spectra was carried out. The best fittings, according to an analysis based on the χ^2 distribution,[19] led to the results shown in Figure 5.

These results are compatible with a CdSe crystal of 5.2 nm and a CdZnS shell of 1.5 nm thick.

In summary, we use the MEIS technique to characterize a core-shell nanostructure of CdSe/ZnS QDs. The crystal size of 5.2 nm, determined by MEIS, is in good agreement with optical measurements and TEM images. The core-shell structure is resolved by the present configuration of MEIS in contrast to the present TEM measurements. The studied QDs present a non-stoichiometric Cd:Se ratio of 0.69:0.31. Our investigation shows the presence of Cd in the shell and a stoichiometric CdSe core. This study shows that the MEIS technique, combined with other analytical techniques, is a powerful method to determine elemental distribution profiles, inside nanoparticles with diameter about 5 nm. The advantage of MEIS over EXAFS/DAFS is the simplicity of the data analysis. This allows for studies of the formation and stability of the internal structure of the QDs when exposed to several kind of processes, like heating and ion irradiation.

The authors acknowledge the financial support by brazilian agencies CNPq, CAPES, FAPERGS, PRONEX program, and the use of the infrastructure of CME-UFRGS.

[1]I. Fortunati, R. Signorini, R. Bozio, J. J. Jasieniak, A. Antonello, A. Martucci, G. D. Giustina, G. Brusatin, and M. Guglielmi, J. Phys. Chem. C **115**, 3840 (2011).
[2]W. K. Chu, J. W. Mayer, and M.-A. Nicolet, *Backscattering Spectrometry* (Academic Press, Orlando, 1978).
[3]E. Gusev, H. Lu, T. Gustafsson, and E. Garfunkel, Phys. Rev. B **52**, 1759 (1995).

[4]M. Copel, IBM J. Res. Dev. **44**, 571 (2000).
[5]M. Copel, S. Oida, A. Kasry, B. A. A., J. Hannon, and R. Tromp, Appl. Phys. Lett. **98**, 113103 (2011).
[6]M. A. Sortica, P. L. Grande, G. Machado, and L. Miotti, J. Appl. Phys. **106**, 114320 (2009).
[7]H. Matsumoto, K. Mitsuhara, A. Visikovskiy, T. Akita, N. Toshima, and Y. Kido, Nucl. Instrum. Methods Phys. Res. B **268**, 2281 (2010).
[8]J. Gustafson, A. R. Haire, and C. J. Baddeley, Surf. Sci. **605**, 220 (2011).
[9]S. J. Rosenthal, J. McBride, S. J. Pennycook, and L. C. Feldman, Surf. Sci. Rep. **62**, 111 (2007).
[10]S. Gapoenko, *Optical Properties of Semiconductor Nanocrystals* (Cambridge University, Cambridge, 1998).
[11]N. Barradas, A. K, G. Battistig, M. Bianconi, N. Dytlewski, C. Jeynes, E. Kótai, G. Lulli, M. Mayer, E. Rauhala, E. Szilágyi, and M. Thompson, Nucl. Instrum. Methods Phys. Res. B **262**, 281 (2007).
[12]See supplementary material at http://dx.doi.org/10.1063/1.4734686 for PowerMeis user's manual.
[13]J. L. Campbell, N. I. Boyd, N. Grassi, P. Bonnick, and J. A. Maxwell, Nucl. Instrum. Methods Phys. Res. B **268**, 3356 (2010).
[14]J. F. Ziegler, J. P. Biersack, and M. D. Ziegler, *SRIM, The Stopping and Range of Ions in Matter* (Chester, Maryland, 2008).
[15]Q. Yang, D. J. O'Connor, and Z. Wang, Nucl. Instrum. Method Phys. Res. B **61**, 149 (1991).
[16]P. L. Grande, A. Hentz, R. P. Pezzi, I. J. R. Baumvol, and G. Schiwietz, Nucl. Instrum. Methods Phys. Res. B **256**, 92 (2007).
[17]M. Hazama, Y. Kitsudo, T. Nishimura, Y. Hoshino, P. L. Grande, G. Schiwietz, and Y. Kido Phys. Rev. B **78**, 1 (2008).
[18]E. Piskorska-Hommel, V. Holý, O. Caha, A. Wolska, A. Gust, C. Kruse, J. Falta, and D. Hommel, J. Alloys Compd. **523**, 155 (2012).
[19]R. Bevington and D. Robinson, *Data Reduction and Error Analysis for the Physical Sciences*, 3rd ed. (Mc Graw Hill, New York, 2003).